

High-quality Single Crystal Growth and Anisotropic Magnetic Properties of UIr

Etsuji YAMAMOTO¹, Yoshinori HAGA¹, Akio NAKAMURA^{1,2}, Yoshihumi TOKIWA^{1,3}, Dai AOKI³,
Rikio SETTAI³ and Yoshichika ŌNUKI^{1,3}

¹Advanced Science Research Center, Japan Atomic Energy Research Institute, Tokai, Ibaraki 319-1195, Japan

²Department of Material Science, Japan Atomic Energy Research Institute, Tokai, Ibaraki 319-1195, Japan

³Graduate School of Science, Osaka University, Toyonaka, Osaka 560-0043, Japan

We succeeded in growing a high-quality single crystal of UIr with the monoclinic structure by the Czochralski pulling method in a tetra-arc furnace. A typical size of an ingot was 2.5 mm in diameter and 65 mm in length. The residual resistivity ratio ρ_{RT}/ρ_0 was 150. The magnetization indicates Ising-like ferromagnetism with a Curie temperature $T_C=46$ K. The easy axis in the magnetization is close to the $[10\bar{1}]$ direction in the b- or (010) plane. A saturated moment is about $0.5 \mu_B/U$. Moderately heavy carriers with the cyclotron effective masses of 9-19 m_0 were detected by the de Haas-van Alphen experiment, which is consistent with the electronic specific heat coefficient $\gamma=48.5$ mJ/K²·mol.

KEYWORDS: magnetization, specific heat, dHvA, UIr

§1. Introduction

Uranium intermetallic compounds indicate many interesting properties including magnetic and quadrupole orderings, heavy fermions and unconventional superconductivity. These properties are closely related to the 5f electrons.¹⁾

The 3d electrons in the transition metals such as Ni and Fe are responsible for ferromagnetism, which was initially discussed on the basis of the localized 3d-electron model. Later studies clarified that the magnetism can be described by the itinerant 3d-electron model. In particular, the experimental Fermi surface studies agree very satisfactorily with the results of energy band structure calculations based on the itinerant 3d-electron model.

On the other hand, the localized picture of 4f electrons in the rare earth compounds is a good starting point to understand their magnetic properties, which are understood on the basis of the well-known RKKY interactions. In some compounds such as CeRu₂Si₂ and CeCu₆, however, the 4f electrons hybridize significantly with the conduction electrons with a wide energy band, which leads to heavy fermions with extremely large electronic specific heat coefficient via the many-body Kondo effect. The 4f electrons become thus itinerant with decreasing the temperature. The crossover from localized to itinerant occurs below the Kondo temperature T_K , which is about 5 K in CeCu₆, for example.

In many aspects, however, the 5f electrons in the uranium compounds, are different from those in the rare earth compounds. For example, the magnetic ordering temperature is widely dispersive, depending on the uranium compound, which is in the range from about 1 K to 300 K. This is in contrast to about 5 K in the cerium compounds. The corresponding magnetic moment ranges from close to zero to $3 \mu_B/U$. This is most likely based on the fact that the 5f electrons in the uranium atom

have an intermediate character between the 3d and 4f electrons, and are located partially inside the closed 6s and 6p shells. Consequently, they sometimes appear to possess dual nature, both localized and itinerant.

There are several intermetallic uranium compounds, which order ferromagnetically. Curie temperatures and saturated moments are, for example, as follows: 125 K ($3.0 \mu_B/U$) in UGa₂,²⁾ 52 K ($1.4 \mu_B/U$) in UGe₂,³⁾ 198 K ($1.82 \mu_B/U$) in U₃As₄,⁴⁾ and 138 K ($1.34 \mu_B/U$) in U₃P₄.⁴⁾

UIr is also a ferromagnet with the monoclinic structure, as shown in Fig. 1. The Curie temperature T_C is 46 K and a saturated moment is $0.5 \mu_B/U$.⁵⁾ The magnetic susceptibility of the polycrystalline sample of UIr obeys the Curie-Weiss law above 500 K, yielding an effective magnetic moment $3.6 \mu_B/U$ and a large negative paramagnetic Curie temperature $\theta_p=-430$ K, which

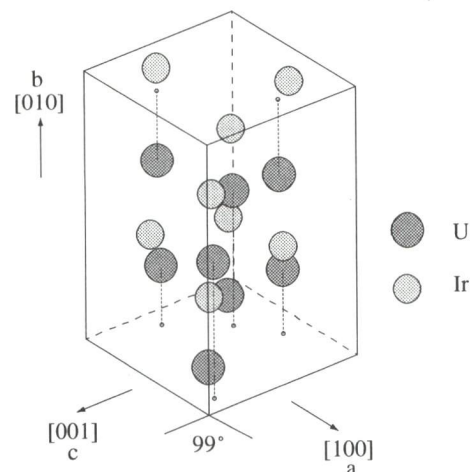


Fig.1. crystal structure of UIr.

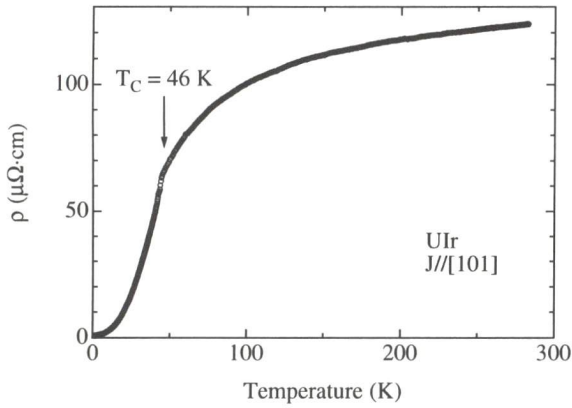


Fig. 2. Temperature dependence of electrical resistivity of UIr.

corresponds to 3.62 (3.58) μ_B/U in the $5f$ -localized $5f^3(5f^2)$ configuration, respectively.

Previously we studied the magnetic property of a polycrystalline sample.⁶⁾ We have continued in growing a single crystal and in studying the electrical and magnetic properties. In this paper, we present the experimental results of electrical resistivity, magnetization, de Haas-van Alphen (dHvA) effect and specific heat in the single crystal of UIr.

§2. Experimental

From the view point of the alloy phase diagram, it is difficult to grow a single crystal of UIr because the melting point of UIr_3 , 2278 K, is higher than that of UIr, 1743 K, and melting point seems to increase as the concentration of Ir increases near UIr. UIr, however, melts congruently. This is the reason why we succeeded in growing a single crystal by the Czochralski method in a tetra-arc furnace. The pulling speed was 14 mm/hour. The ingot was 2.5 mm in diameter and 65 mm in length. The crystal was grown along the [101] direction.

The electrical resistivity was measured by the conventional four-probe DC method. The magnetization was measured by the commercial SQUID magnetometer. The specific heat measurement was done by the quasi-adiabatic heat-pulse method. The dHvA experiment was done by the usual field modulation method in magnetic fields up to 170 kOe and at low temperatures down to 30 mK.

§3. Results and Discussion

Figure 2 shows the temperature dependence of the electrical resistivity for the current along the [101] direction. The resistivity indicates a T^n ($n \leq 1$)-dependence in the paramagnetic region, which is characteristic in the uranium compounds. A steep decrease below 46 K is due to the ferromagnetic ordering, as mentioned in §1. The resistivity follows a T^2 -dependence below 12 K: $\rho = \rho_0 + AT^2$ ($\rho_0 = 0.7 \mu\Omega\cdot\text{cm}$ and $A = 1.74 \times 10^2 \mu\Omega\cdot\text{cm}/\text{K}^2$). The residual resistivity ratio (ρ_{RT}/ρ_0) was 150, indicating a high-quality sample.

Next we measured the magnetization at 2 K. Figure 3 shows the magnetization curves for three typical directions. Contrary to the previous result,⁵⁾ the easy axis

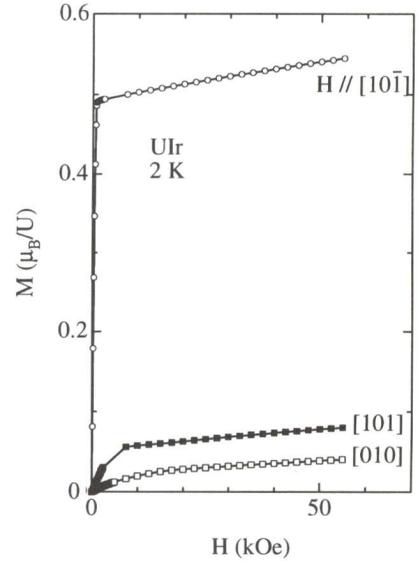


Fig. 3. Magnetization curves of UIr.

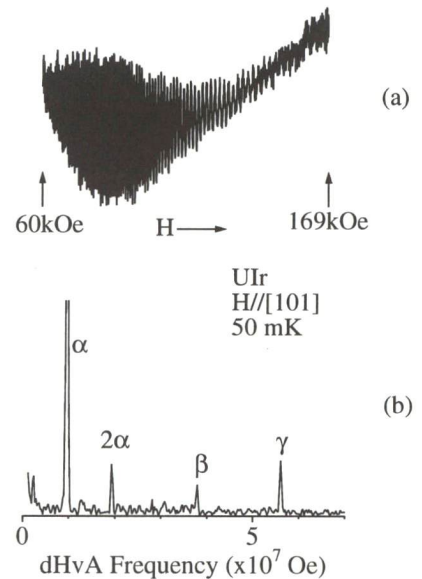


Fig. 4. (a) Typical dHvA oscillation and (b) the corresponding FFT spectrum for the field along the [101] direction.

in the magnetization is found not to be the [010] direction but to be close to the $[10\bar{1}]$ direction in the b - or (010) plane because the [101] direction, which is almost perpendicular to $[10\bar{1}]$, contains 10 percent of a ferromagnetic contribution, compared to $[10\bar{1}]$. The magnetization along [010], which is perpendicular both $[10\bar{1}]$ and [101], indicate the usual hard-axis behavior.

We measured the dHvA effect in magnetic fields up to 170 kOe and at temperatures down to 30 mK. Figure 4 shows the typical dHvA oscillation and the corresponding fast Fourier transform (FFT) spectrum for the field along the [101] direction. Three dHvA branches, named α , β and γ as well as the second harmonic of the branch α are observed clearly.

Here, the dHvA voltage V_{osc} is obtained in the so-

called 2ω detection of the field modulation method, following the Lifshitz-Kosevich formula:

$$V_{\text{osc}} = A \sin\left(\frac{2\pi p F}{H} + \phi\right), \quad (3.1)$$

$$A \propto J_2(x) T H^{-1/2} \frac{\exp(-\alpha p m_c^* T_D/H)}{\sinh(\alpha p m_c^* T/H)}, \quad (3.2)$$

$$\alpha = \frac{2\pi^2 k_B c}{e\hbar} \quad (3.3)$$

and

$$x = \frac{2\pi p F \hbar}{H^2}, \quad (3.4)$$

where $J_2(x)$ is the Bessel function which depends on the dHvA frequency F , the modulation field h and magnetic field strength H . The dHvA frequency $F (= \hbar c S_F / 2\pi e)$ is proportional to the extremal (maximum or minimum) cross-sectional area S_F of the Fermi surface, m_c^* is the cyclotron effective mass and $T_D (= \hbar / 2\pi k_B \tau)$ is the Dingle temperature which is inversely proportional to the scattering lifetime of the conduction electron τ .

From the angular dependence of the dHvA frequency, it is found that branch α corresponds to a nearly spherical Fermi surface and branches β and γ , which are observed around $[101]$, are due to a multiply-connected Fermi surface.

We determined the cyclotron mass from the temperature dependence of the dHvA amplitude: $9.4 m_0$ for branch α with the dHvA frequency of 9.65×10^6 Oe, $16 m_0$ for β with 3.79×10^7 Oe and $19 m_0$ for γ with 5.60×10^7 Oe. These results indicate that the present carriers are moderately heavy, which is mainly due to the itinerant $5f$ electrons.

We also determined the Dingle temperature from the field dependence of the dHvA amplitude: $T_D = 0.20$ K for branch α , 0.25 K for branch β and 0.37 K for branch γ .

From the simple relations:

$$S_F = \pi k_F^2, \quad (3.5)$$

$$\hbar k_F = m_c^* v_F, \quad (3.6)$$

and

$$l = v_F \tau, \quad (3.7)$$

where k_F is half of the caliper dimension of circular S_F , and v_F is Fermi velocity, we can estimate the mean free path l : $l = 1270 \text{ \AA}$ for branch α , 1200 \AA for branch β and 840 \AA for branch γ . A value of about 1000 \AA is relatively large, indicating a high-quality sample.

Finally we determined the specific heat coefficient γ . Figure 5 shows the T^2 dependence of the specific heat C

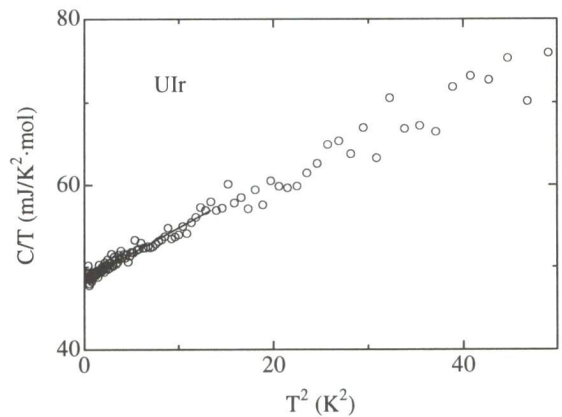


Fig. 5. Temperature dependence of the specific heat C .

in the form of C/T . The electronic specific heat coefficient is obtained as $\gamma = 48.5 \text{ mJ/K}^2 \cdot \text{mol}$. This γ value is consistent with the large cyclotron mass mentioned above.

§4. Summary

We grew a high-quality single crystal of UIr and measured the electrical resistivity, magnetization, de Haas-van Alphen oscillation and specific heat. We summarize our experimental results.

- (1) The easy axis in the magnetization is found to be close to the $[10\bar{1}]$ direction. This is different from the previous result of the $[010]$ direction.
- (2) Three dHvA branches are detected. The cyclotron mass is in the range from 9 to $19 m_0$.
- (3) This large mass is consistent with the electronic specific coefficient $\gamma = 48.5 \text{ mJ/K}^2 \cdot \text{mol}$.

Acknowledgements

This work was supported financially by the Grant-in-Aid for COE Research (10CE2004) from the Ministry of Education, Science, Sports and Culture.

- 1) Y. Ōnuki, T. Goto and T. Kasuya: *Mater. Sci. Technol.* **A3** (1992) 545.
- 2) T. Honma, Y. Inada, R. Settai, S. Araki, Y. Tokiwa, T. Takeuchi, H. Sugawara, H. Sato, K. Kuwahara, M. Yokoyama, H. Amitsuka, T. Sakakibara, E. Yamamoto, Y. Haga, A. Nakamura, H. Harima, H. Yamagami and Y. Ōnuki: *J. Phys. Soc. Jpn.* **69** (2000) 2647.
- 3) J. J. M. Franse: *High Field Magnetism*, ed. M. Date (North-Holland, Amsterdam) (1983) p.189.
- 4) P. Wiśniewski, A. Gukasov and Z. Henkie: *Phys. Rev* **B60** (1999) 6242.
- 5) A. Dommann, F. Hulliger, T. Siegrist and P. Fischer: *J. Magn. Magn. Mater.* **67** (1987) 323.
- 6) Y. Ōnuki, S. W. Yun, I. Ukon, A. Kobori, I. Umehara, K. Satoh, T. Fukuhara, H. Sato and S. Takayanagi: *J. Phys. Soc. Jpn.* **61** (1991) 1751.